Freezing-induced topological transition of double-emulsion (Supplemental Material)

Jochem G. Meijer,[1] Pallav Kant,[2] and Detlef Lohse[1,3]

[1] *Physics of Fluids group, Max Planck Center Twente for Complex Fluid Dynamics, Department of Science and Technology, Mesa+ Institute and J. M. Burgers Center for Fluid Dynamics, University of Twente, P.O. Box 217, 7500 AE Enschede, The Netherlands*
[2] *School of Engineering, University of Manchester, M13 9PL, United Kingdom*
[3] *Max Planck Institute for Dynamics and Self-Organization, Am Faßberg 17, 37077 Göttingen, Germany*

(Dated: January 31, 2024)

List of Supplementary Movies

- **Movie 1:** Movie showing the complete engulfment process of a compound droplet into the ice and the sudden topological transition, where the front advances at a velocity $V = 0.5\,\mu\mathrm{m\,s^{-1}}$. Snapshots are taken at a low frame rate of 0.25 frames/sec. The movie corresponds to Fig. 2(a)(1-5) of the main text.
- **Movie 2:** The sudden topological transition of a compound droplet completely surrounded by ice captured through high-speed imaging at 25.000 frames/sec. To ensure good optical resolution the field of view of the camera is limited and the moving solidification front can therefore not be captured simultaneously. The movie corresponds to Fig. 2(a)(I-IV) of the main text.
- **Movie 3:** The sudden topological transition of a compound droplet completely surrounded by ice captured through high-speed imaging at 75.000 frames/sec. To ensure good optical resolution the field of view of the camera is limited and the moving solidification front can therefore not be captured simultaneously.
- **Movie 4:** The dissolution of the inner drop of a barely stable compound droplet ($R_{\mathrm{in}} > 30\,\mu\mathrm{m}$) that is partially engulfed into the ice. The process is captured through high-speed imaging at 10.000 frames/sec. The movie corresponds to Fig. 3(a) of the main text.

General Experimental Details

In this section we address some general experimental details and technicalities in more detail. The preparation of the double-emulsion is discussed specifically in the following section. The exact protocol adopted in our current investigations is as follows. At the beginning of each experiment, the Hele-Shaw cell (Ibidi, μ-Slide I Luer) is placed on a copper block maintained at a fixed thermal gradient and the double-emulsion is injected. We then initiate the solidification on the colder end of the Hele-Shaw cell by inserting a small piece of ice, that acts as nucleation site and hence prevents the liquid to become supercooled. After the initialization, a solidification front forms that slowly advances into the field of view of the camera. This can take easily up to an hour. To capture the entire engulfment process we use a Nikon D850 camera with long working distance lens (Thorlabs, MVL12X12Z) plus 2X lens attachment. The working distance of the objective is 37 mm and 1 picture is taken every four seconds. To visualise the sudden topological transition we use a high-speed camera (Photron NOVA S16) with the same objective and a frame-rate up to 75.000 fps (Supplementary Movie 3). The upper limit of the frame-rate is set by the amount of available back-light (Schott KL2500).

If the slide remained stationary, the front keeps advancing until it has propagated out of view. Alternatively, we can set the Hele-Shaw cell slide in motion with velocity V, opposite to the direction of motion of the solidification front, using a linear actuator (Physik Instrumente, M-230.25). The lowest velocity that was measured at which the slide can be pushed is $V = 0.1\,\mu\mathrm{m\,s^{-1}}$. The calibration measurements verified that at this velocity the variations are within 25%. When increasing the velocity the stability increases and the variations fall within 10% for $V = 0.4\,\mu\mathrm{m\,s^{-1}}$ and beyond. By properly choosing V it will appear as if the front remains stationary and that the droplets approach the front, whereas in reality it is vice versa. We therefore can change V by changing G. To correct for irregularities in environmental heat losses, that slightly alter the growth rate of the ice, the voltage of the Peltier element on the colder side is continuously adjusted. We do so to ensure that the solidification front remains stationary in our laboratory

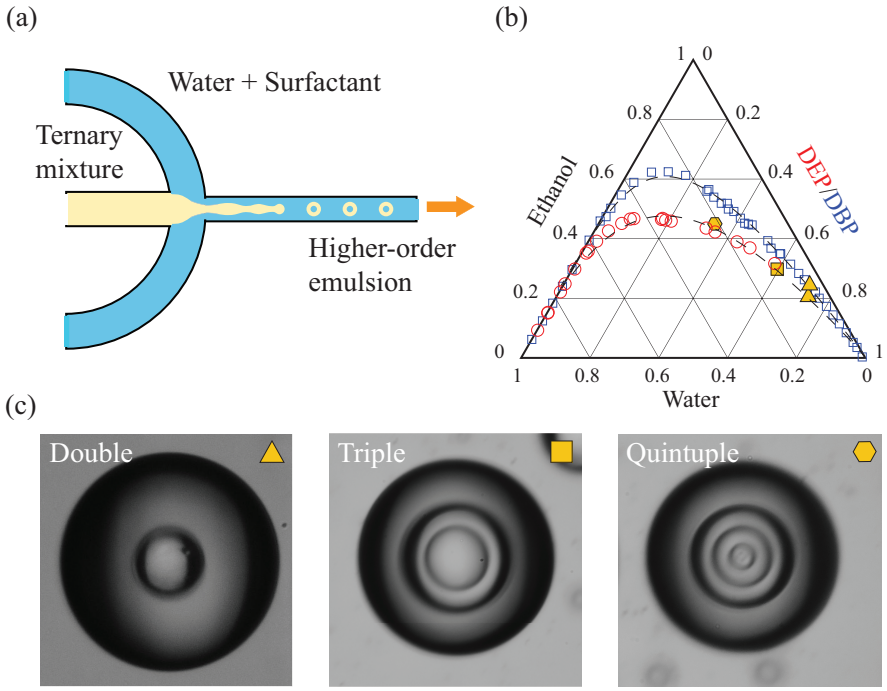

Supplementary Figure 1. (a) Schematic representation of the microfluidic device used to prepare the double-emulsion. the widths of the channels are approximately 0.7 mm. (b) Ternary phase diagram showing the binodal line of the ethanol/water/DEP (red) and ethanol/water/DBP (blue) systems [3]. Yellow symbols indicate the approximate initial composition of the ternary ethanol/water/DEP mixture to obtain a double-, triple or quintuple-compound droplet (c), respectively. For our current study we use an initial composition of (0.21/0.05/0.74 vol.) for the ethanol/water/DEP system and (0.218/0.032/0.75 vol.) for the ethanol/water/DBP system.

framework. Thus, although V and G can be altered independently, we chose to perform experiments in a manner that the velocity of the freezing front is determined by the applied thermal gradient.

Preparation of double-emulsion

Here we discuss the preparation of the double-emulsion in more detail. It is inspired by prior work [1, 2]. The double-emulsion is prepared using a 3D-printed microfluidic chip, schematically represented in Supplementary Fig. 1(a). Typically, for the preparation of single-emulsions, one uses a bulk phase (Milli-Q water) and a dispersed phase (oil). Dependent on the flow rates of both phases through the microfluidic channels, a jet is formed that destabilises and thus produces sub-milimetric sized drops. Here, the oil is replaced by a ternary mixture of ethanol (Sigma-Aldrich, Germany), water (Milli-Q water) and diethyl phthalate (DEP) (Sigma-Aldrich, Germany), where the melting temperature of DEP is $T_{\mathrm{m,DEP}} = -3\,^{\circ}\mathrm{C}$. Suitable flow rates are $Q = 8\,\mathrm{mL\,min^{-1}}$ for the outer water phase and $Q = 0.5\,\mathrm{mL\,min^{-1}}$ for the dispersed ternary mixture.

To ensure stability a surfactant Pluronic-F127 (Sigma-Aldrich, Germany) is added to the water. In the initial phase of our study samples were prepared using different concentrations and dilutions to study the effect the surfactant concentration might have on the observations. For the dilutions that were considered we have observed that too few surfactant (0.01 wt%) significantly reduces the lifetime of the compound droplets in the double-emulsion and too much surfactant (1 wt%) causes the freezing front to become unstable. The latter is also greatly affected by the amount of ethanol in the system. For our current study we have chosen an initial surfactant concentration of 0.1 wt%. At the beginning of the experiment, before the sample is injected into the Hele-Shaw cell, it is diluted ten times with water (Mili-Q water) to ensure that the traces of ethanol in the system do not affect the stability of the growing crystal. The diluted double-emulsion sample remained stable for several days.

Dependent on the initial concentration of the ternary liquid, the drops that pinch off from the jet stabilise into higher order emulsions through liquid-liquid phase separation [1]. Supplementary Fig. 1(b) shows the ternary diagram of the ethanol/water/DEP system [3]. The different symbols indicate the approximate initial concentration of the ternary

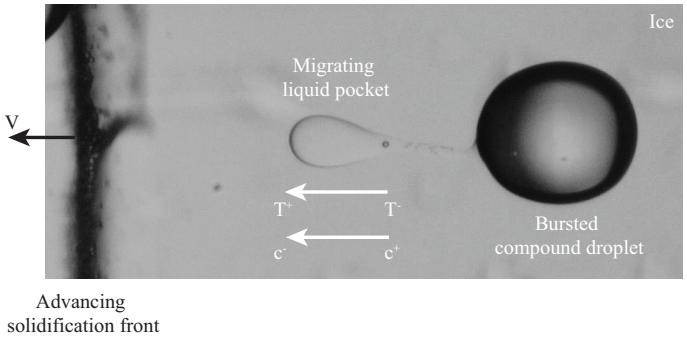

Supplementary Figure 2. Liquid pocket migration of the expelled interior through the ice. The applied thermal gradient induces a concentration gradient. While diffusion restores this concentration gradient, the local phase equilibrium at the colder and warmer sides are altered leading to the migration. Eventually, the pocket catches up with the ice front, which propagates with velocity V.

liquid and the double-, triple- and quintuple-emulsions that are produced; see Supplementary Fig. 1(c). For our current study we have chosen an initial condition of (0.21/0.05/0.74 vol.) for ethanol, water and DEP, respectively, and hence focus on double-emulsions only.

Liquid pocket migration

As discussed in the main text, after the topological transition has taken place, the expelled liquid accumulates at the warmer end of the engulfed droplet, before migrating at a constant migration velocity $|v_{\mathrm{diff}}| \approx 1 - 3\,\mu\mathrm{m\,s^{-1}}$ through the solidified bulk in the direction of motion of the solidification front, see Supplementary Fig. 2. Recalling that the expelled water drop contains traces of ethanol and given the applied temperature gradient, we argue that the migration process is equivalent to the process of brine pockets migrating through sea ice, i.e., 'brine pocket diffusion' [4–6]. The driving force for such migration originates from the gradient in composition over the pocket, which is governed by the applied thermal gradient $\mathrm{d}T/\mathrm{d}x$ and concentration dependence on temperature, $\mathrm{d}c/\mathrm{d}T$, given by its phase diagram. Under steady-state conditions, the flux of ethanol c within the pocket is driven by diffusion. Due to this diffusion, the local compositions vary, as do the local, composition-dependent melting temperatures. This causes water to freeze at the colder side and ice to melt at the warmer side. The velocity at which the water-ethanol pocket migrates, v_{diff}, is thus given by a simple diffusion equation, $c\,v_{\mathrm{diff}} = -D\,\mathrm{d}c/\mathrm{d}x$, where $\mathrm{d}c/\mathrm{d}x = (\mathrm{d}c/\mathrm{d}T)(\mathrm{d}T/\mathrm{d}x)$. Hence,

$$\left|\frac{\mathrm{d}\delta}{\mathrm{d}t'}\right| = |v_{\mathrm{diff}}| = -\frac{D}{c}\frac{\mathrm{d}c}{\mathrm{d}T}G, \tag{S.1}$$

where D is the solute diffusivity, $\mathrm{d}T/\mathrm{d}x = G$ the applied thermal gradient and c the ethanol concentration within the migrating volume. Considering that $D \sim 1 \times 10^{-9}\,\mathrm{m^2\,s^{-1}}$, $c \sim 0.02$, $\mathrm{d}c/\mathrm{d}T \sim -0.02\,\mathrm{K^{-1}}$ and $G \sim 5\,\mathrm{K\,mm^{-1}}$ yields $|v_{\mathrm{diff}}| \sim 5\,\mu\mathrm{m\,s^{-1}}$, which agrees with the values observed experimentally.

Light intensity increase during bursting

The captured high-speed images reveal that during the radial expansion of the spherical dark feature a local increase in light intensity is observed. The behaviour of the mean light intensity during one bursting event is measured and shown in Supplementary Fig. 3. When the dark feature first appears in the center of the inner drop, the intensity slightly decreases (I). Then the mean intensity rapidly increases together with the expanding ring until its size coincides with the size of the inner drop (II), where a second minor decrease in intensity is measured (III). Finally, the intensity reaches a certain maximum (IV) before slowly decaying towards an equilibrium value.

The origin of this overshoot in light intensity, we argue, is the change in optical path of the back-light as the ethanol vapour cloud expands, allowing more light to pass through to the camera without being deflected. The interior of the drop thus appears brighter due to the lower index of reflection of the vapour.

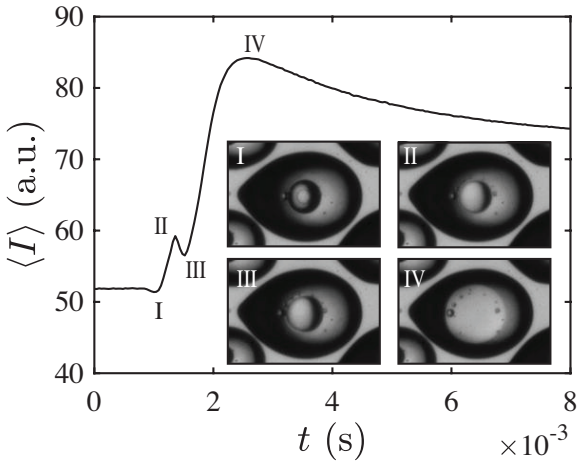

Supplementary Figure 3. Mean of the light intensity captured during the topological transition. The inset shows the corresponding experimental snapshots.

Repeating experiments with dibutyl phthalate (DBP)

To verify whether the partial solidification of the oil phase indeed triggers the topological transition, the experiments are repeated by replacing DEP with dibutyl-phthalate (DBP), that has similar properties compared to DEP but a significantly lower melting temperature, i.e., $T_{\mathrm{m,DBP}} = -35\,^{\circ}\mathrm{C}$. These temperatures can not be achieved in our experimental setup. The phase diagram of the ethanol/water/DBP system is shown in Supplementary Fig. 1 [3]. The initial concentration is (0.218/0.032/0.75 vol.) for ethanol, water and DBP, respectively. During the performed experiments using this system, no sudden topological transition of the double-emulsion was observed.

Freezing of a more densely packed double-emulsion

Our current study focusses on the freezing of a dilute double-emulsion, meaning that the dispersed compound droplets are virtually isolated to study the behaviour of individual droplets that are being approached by an advancing solidification front. When considering the freezing of a more densely packed double-emulsion, where compound droplets are closely together (see Supplementary Fig. 4), we observe the same phenomena as discussed in the main text for those compound drops where $R_{\mathrm{in}} > R_{\mathrm{in,crit}}$, once they are incorporated in the ice and the front has advanced far enough (see red rectangles in Supplementary Fig. 4).

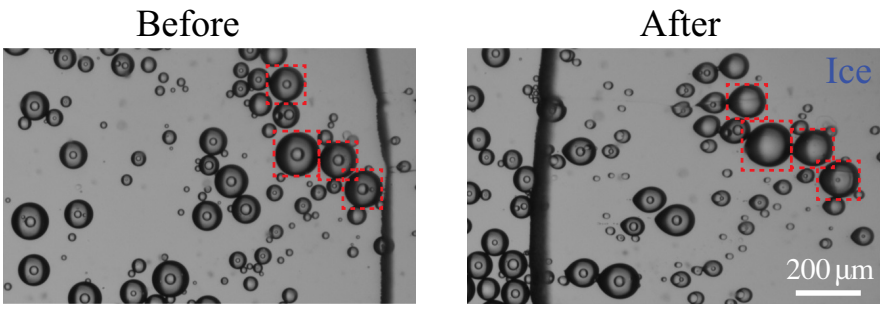

Supplementary Figure 4. Experimental snapshots of before and after the freezing of a more densely packed double-emulsion. The compound droplets incorporated in the ice for which $R_{\mathrm{in}} > R_{\mathrm{in,crit}}$ will eventually expel their inner core (see red rectangles).

REFERENCES

[1] Martin F Haase and Jasna Brujic, "Tailoring of high-order multiple emulsions by the liquid–liquid phase separation of ternary mixtures," Angewandte Chemie **126**, 11987–11991 (2014).

[2] Pepijn G Moerman, Pierre C Hohenberg, Eric Vanden-Eijnden, and Jasna Brujic, "Emulsion patterns in the wake of a liquid–liquid phase separation front," Proceedings of the National Academy of Sciences **115**, 3599–3604 (2018).

[3] Magdalena Bendová, Karel Řehák, Jaroslav Matouš, and Josef P Novák, "Liquid+ liquid equilibrium in the ternary systems water+ ethanol+ dialkyl phthalate (dimethyl, diethyl, and dibutyl phthalate) at 298.15 k," Journal of Chemical & Engineering Data **46**, 1605–1609 (2001).

[4] WG Whitman, "Elimination of salt from sea-water ice," American Journal of Science **5**, 126–132 (1926).

[5] Pieter Hoekstra, Thomas E Osterkamp, and Wilford Frank Weeks, "The migration of liquid inclusions in single ice crystals," Journal of Geophysical Research **70**, 5035–5041 (1965).

[6] JD Harrison, "Measurement of brine droplet migration in ice," Journal of Applied Physics **36**, 3811–3815 (1965).